Shape and Compound Elastic Scattering of α Particles by ^{40}Ca, 5.0 to 12.5 MeV*

JOSEPH JOHN,† C. P. ROBINSON,‡ J. P. ALDRIDGE, AND R. H. DAVIS
Department of Physics, Florida State University, Tallahassee, Florida 32306

(Received 23 August 1968)

The differential cross section for the elastic scattering of α particles by ^{40}Ca has been measured at sixteen angles between 5.0 and 12.5 MeV in 10-keV intervals. Complicated structure is seen in the excitation functions which is often as fine as the experimental resolution (<10 keV). There are many closely spaced anomalies which are substantially wider than the experimental resolution. Very broad undulations are apparent in averaged differential cross-section curves for which the averaging interval is about 0.5 MeV. The averaged data are analyzed in this work. Shape elastic scattering represented by an optical model where reaction channels are either closed or strongly inhibited does not satisfactorily describe the angular distributions at the back angles. A combination of shape and compound elastic scattering reproduces the data except at the highest energies, where reaction cross sections are becoming significant. The expression for the compound elastic contribution to the cross section is based on Hauser-Feshbach theory and statistical-model considerations. Values obtained for the real potential-well depth of the optical model (~140 MeV) are consistent with results previously obtained at higher energies for the same number of nodes in the s-wave function.

I. INTRODUCTION

UNTIL recently, information on the elastic scattering of α particles by ^{40}Ca below 20 MeV has been scarce. Brady *et al.*[1] measured the differential cross section at 30 angles at the three isolated energies 8.71, 9.29, and 10.10 MeV. Bock *et al.*[2] studied the angular distribution at the single energy of 19.47 MeV. These measurements showed a marked increase in the cross section at backward angles which was not so evident in the data for other nuclei in the same mass region. Only limited attempts were made at fitting data using the optical model.

Several experiments have been performed at energies above 25 MeV. Gruhn and Wall[3] studied the reaction between 27.0 and 42.0 MeV, using the α-particle beam from a cyclotron. While the forward-angle data displayed the usual diffraction pattern, the large-angle cross sections showed an oscillatory pattern in which the last few maxima remained relatively fixed in angle as the energy was changed. The optical model produced a reasonable fit at forward angles, but its predictions fell considerably below the experimental values at back angles. This discrepancy could not be accounted for by either an exchange process or virtual excitation. On the other hand, using a modified Blair smooth cutoff model, these authors were able to qualitatively describe this large-angle behavior. The main feature of this calculation was the inclusion of a term in the scattering amplitude representing a resonance due to a compound nucleus state.

Between 30 and 40 MeV, Boschitz *et al.*[4] studied the large angle scattering of α particles by ^{40}Ca and compared it to the scattering from ^{16}O, ^{28}Si, ^{32}S, ^{36}Ar, and ^{40}Ar. With the exception of ^{40}Ar, all the data had the common feature of an enhancement of the large-angle cross section with sharp minima which remained stationary with respect to the bombarding energy. The results of experiments by Budzanowski *et al.*[5] consist of six angular distributions between 23.37 and 28.92 MeV. Satisfactory optical-model fits could be obtained only after modifying the phase shift corresponding to the $l=10$ partial wave to include a single level resonance. The existence of a broad $J=10^+$ resonance at about 24.1 MeV is indicated by the analysis.

The most comprehensive experiments have been performed recently by Robinson *et al.*[6] covering the energy range 12.0–18.0 MeV. Sixteen-point angular distributions were measured every 25 keV and 64-point angular distributions every 100 keV throughout this energy range. Good fits to the detailed angular distributions were obtained with the optical model using a Woods-Saxon real potential and a surface imaginary potential with a form given by the derivative of the Woods-Saxon function. Fits to the back-angle data were improved by employing a quantity g^2 as the criterion for describing the quality of the fit instead of the quantity χ^2 commonly used. Calculated cross sections at the back angles are brought closer to the experimental values by this technique, in which the points are weighted by the

* Supported in part by the Air Force Office of Scientific Research, Office of Aerospace Research, U.S. Air Force under AFOSR Grant No. AF-AFOSR-440-67 and in part by National Science Foundation Grant No. NSF-GP-5114.

† Present address: Gulf General Atomics, Inc., San Diego, Calif.

‡ Present address: Los Alamos Scientific Laboratory, Post Office Box 0, Mercury, Nev.

[1] F. P. Brady, J. A. Jungerman, J. C. Young, and P. J. Symonds, Nucl. Phys. **A98**, 241 (1967).

[2] R. Bock, P. David, H. H. Duhm, H. Hefele, U. Lynen, and R. Stock, Nucl. Phys. **A92**, 539 (1967).

[3] C. R. Gruhn and N. S. Wall, Nucl. Phys. **81**, 161 (1966).

[4] E. T. Boschitz, J. S. Vincent, R. W. Bercaw, and J. R. Priest, Phys. Rev. Letters **13**, 442 (1964).

[5] A. Budzanowski, K. Grotowski, L. Jarczyk, H. Niewodniczanski, and A. Strazalkowski, Cracow Institute of Nuclear Physics Report No. 502/PL, 1966, Cracow, Poland (unpublished).

[6] C. P. Robinson, J. P. Aldridge, Joseph John, and R. H. Davis, Phys. Rev. **171**, 1241 (1968).

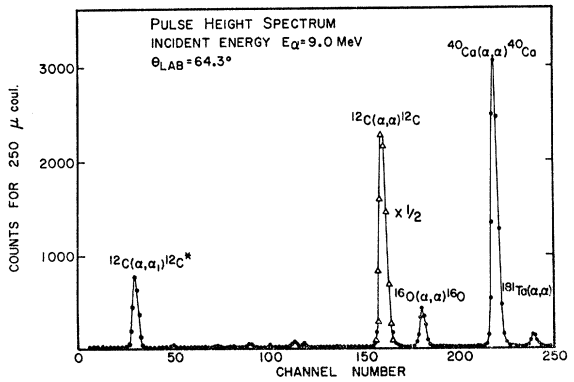

FIG. 1. Pulse-height distribution measured at 64.3°. The peaks are identified by labels placed above each. Tantalum is present as a contaminant.

reciprocal of the Rutherford scattering cross section. The quality of the fits at forward angles was not sacrificed to a significant extent. Three phase-equivalent potentials[7] were traced as functions of energy. The averaged real potential was observed to be relatively constant and the averaged imaginary part to increase with the incident beam energy.

This study is a continuation downward in energy of the work of Robinson *et al.*[6] with the distinction that the elastic scattering is dominant. Below the neutron threshold only the (α, γ) and (α, p) reactions are energetically possible aside from the elastic and inelastic α-particle scattering. Relative to the elastic exit channel, the other compound system decays are inhibited by penetration or transition factors, or are energetically forbidden in the energy range studied here. Under these circumstances the contribution of compound elastic scattering is expected to be significant.

To smooth the excitation functions in preparation for an investigation of the compound elastic-scattering contribution, the measured cross sections have been energy averaged using a Lorentzian weighting function with full width at half-maximum (FWHM) equal to 0.5 MeV. The averaged angular distributions have been fitted using an optical-model program which included a compound elastic contribution added incoherently to the shape elastic cross section. Satisfactory fits are obtained. In contrast, optical-model calculations with no compound elastic term included are in poor agreement with the data, especially at large angles.

II. EXPERIMENTAL PROCEDURE AND RESULTS

The α-particle beam[8] from the Florida State University Tandem Van de Graaff Accelerator was directed onto the target located at the center of an 18-in. diam stainless-steel scattering chamber. The component arrangement in this chamber and general procedures for its use have been previously described.[6]

Thin targets for these measurements were prepared by evaporating natural calcium metal (99.9% pure) from a tantalum boat onto very thin carbon backings. On completion of the evaporation, the calcium targets were allowed to oxidize into a mixture of calcium oxide and calcium hydroxide. These targets were able to withstand α-particle beams as high as 0.5 μA for 5–6 days without showing evidence of any deterioration. In all cases, the total energy loss in the target was held to less than 8 keV. A typical pulse-height distribution is displayed in Fig. 1.

The over-all resolution for each of the 16 detector systems[6] was nearly 120 keV. This included the beam spread, target thickness, kinematical spread over the angular resolution of the detector, preamplifier and amplifier noise, and cross talk between different inputs of the analog-to-digital unit. Corrections for the analyzer dead time were made using the system developed by one of the authors.[9]

Absolute cross sections were determined by normalization of the data to Rutherford scattering at angles forward of 90° at 5.0, 5.1, and 5.2 MeV. At these energies the differential cross section follows the Rutherford scattering angular dependence up to approximately 102°.

Statistical error in the counts was typically 3% in most of the detection systems. At angles where deep minima in the cross section were present, the error may be as high as 6%. A systematic error of 6% has been assigned to the absolute cross-section determination.

The differential cross sections for the elastic scattering of α particles by ^{40}Ca were measured at 16 angles from 26.7° to 176.1° in the c.m. system. These measurements covered the energy range 5.0–12.5 MeV in 10-keV steps. Fourteen of these excitation curves are displayed in Figs. 2 and 3. The data points are denoted by closed circles and these are often jointed by lines to guide the eye. Also shown in these figures are the averaged cross sections which will be discussed in Sec. III.

III. ANALYSIS

The excitation curves vary rapidly with energy at all angles. At forward angles the relative magnitude of the variation is small while at back angles it is comparable to the mean value of the cross section. A dense spectrum of levels in the compound system is evident although not resolved. Because of the difference in scale, the back angle anomalies appear more pronounced than those at forward angles. Certain of the anomalies may be due to individual levels (for example, the anomaly at about 7.27 MeV) but for the most part, the excitation curves show dense fluctuations about an average curve. The description of the average behavior in terms of a potential model is investigated here.

[7] W. J. Thompson, G. E. Crawford, and R. H. Davis, Nucl. Phys. **A98**, 228 (1967).

[8] Joseph John, C. P. Robinson, J. P. Aldridge, W. J. Wallace, K. R. Chapman, and R. H. Davis, Nucl. Instr. Methods **57**, 105 (1967).

[9] Joseph John, Ph.D. dissertation, The Florida State University, 1968 (unpublished).

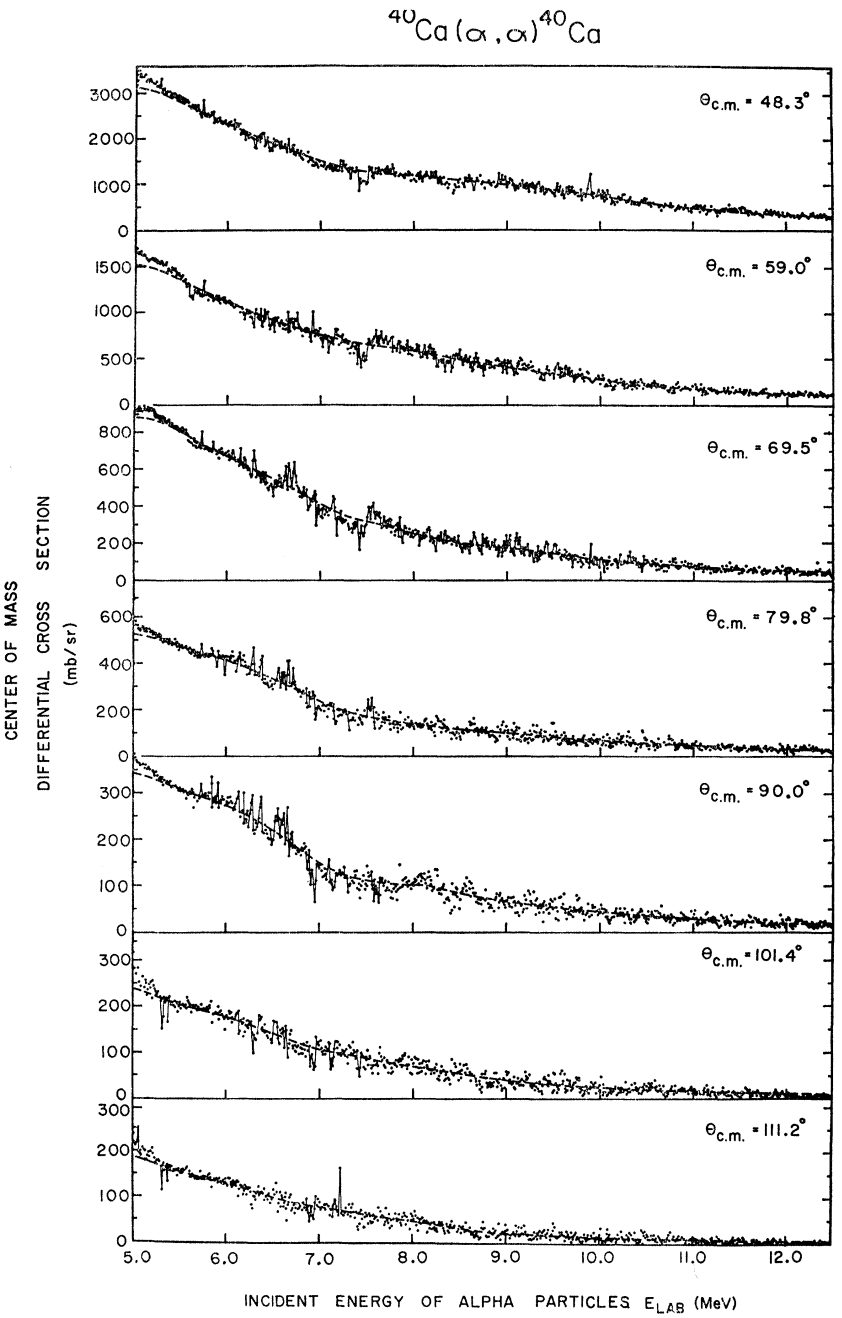

FIG. 2. Excitation function measured at forward and middle angles. Some data points have been joined by lines to guide the eye. The dashed lines are the average cross sections computed from the measured values using a Lorentzian weighting function with a FWHM of 0.5 MeV and a cutoff at 2.0 MeV.

Two purposes are served by the analysis of the data in terms of the nuclear optical model. The first is to extend the study of the energy dependence of the real and imaginary potential strengths keeping the same geometric parameters as those used by Robinson *et al.*,[6] who studied the α-particle scattering by ^{40}Ca from 12.0 to 18.0 MeV. The second purpose is to measure the contribution of the compound elastic-scattering processes to the observed cross section.

To obtain optical-model parameters from high-resolution data in which the cross sections vary rapidly with energy, either the data must be averaged or the parameter sets obtained by fits to high-resolution data must be averaged. The scattering matrix computed using the optical model represents the energy average of the true scattering matrix. This contains no rapidly fluctuating contributions unless additional assumptions are made, as discussed by Aldridge *et al.*[10] and by Robinson *et al.*[6] in analyses of fits to high-resolution data. Because of the density and frequent overlap of the

[10] J. P. Aldridge, G. E. Crawford, and R. H. Davis, Phys. Rev. **167**, 1053 (1968).

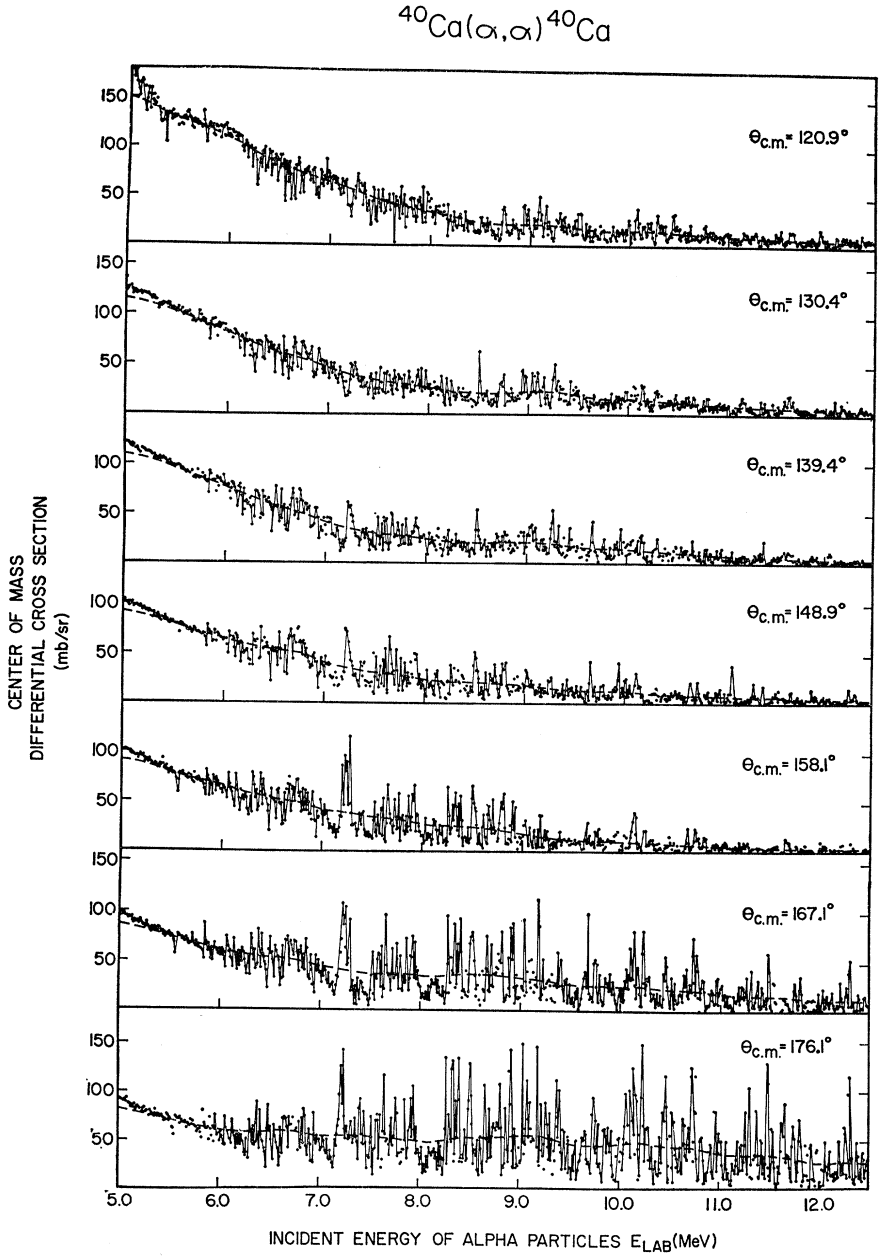

FIG. 3. Excitation functions measured at seven backward angles. The broken line is obtained by smoothing the measured cross section using a Lorentzian weighting function with a FWHM of 0.5 MeV. The continuous lines merely join adjacent data points.

anomalies apparent in the excitation curves, it is assumed that fitting averaged data would yield meaningful optical-model parameters.

The interval over which the high-resolution data were to be averaged was somewhat arbitrary as was the choice of the weighting function. The requirements were that the weighting function have reasonable form, and that the interval be sufficiently large to smooth the fine structure. The experimental cross section at each of the 16 angles were smoothed using a Lorentzian weighting function $\omega(E-E_0)$, defined by

$$\omega(E-E_0)=[I^2/(E-E_0)^2+I^2]. \quad (1)$$

Here the quantity $2I$ represents the FWHM and E_0 is the energy at which the average value was computed. The average cross section $\langle\sigma(E_0)\rangle$ was given by the equation

$$\langle\sigma(E_0)\rangle=\sum_{E_0-\Delta E}^{E_0+\Delta E}\sigma(E)\omega(E-E_0)/\sum_{E_0-\Delta E}^{E_0+\Delta E}\omega(E-E_0), \quad (2)$$

where $\sigma(E)$ is the measured cross section at energy E. The averaging interval $2\Delta E$ was limited to 2.0 MeV. The error in the averaged cross section introduced by the finite range of the averaging interval was estimated to be 1.5%.

In Figs. 2 and 3 the dashed lines represent the averaged values of the cross sections obtained with a weighting function of 0.5 MeV FWHM. A reduction to 0.3 MeV FWHM did not change the results.

Near either end of the energy range covered in this experiment, the averaging interval extended beyond the region where the cross section was measured. In these cases, the averaging was confined to the region in which data were available. Figures 2 and 3 show that the average cross section is consistently lower than the measured cross section in the vicinity of 5.0 MeV. Since the cross section drops below the value of 5.0 MeV as the bombarding energy is increased, the average value obtained at 5.0 MeV is in error and has not been used in any analysis. The "end effect" was not so obvious at 12.5 MeV because the mean value is not changing rapidly with energy.

After the data had been averaged, the angular distributions were found to have very little structure. The large oscillations in the differential cross section, observed in the high-resolution data, were damped and deep minima were no longer present. In addition, the averaged angular distribution at one energy was not significantly different from that observed at an energy a few hundred keV away. Hence it was sufficient to analyze angular distributions every 0.5 MeV to study systematics of the optical-model parameters.

A. Shape Elastic Scattering

The adopted form of the optical-model potential matched the form used by Robinson *et al.*[6] as closely as possible. They found that a volume-absorption potential and a surface-absorption potential described the observed cross section equally well provided that the volume-absorption potential had a radius parameter which was larger than that for the surface-absorption potential. Since all of their analysis employed a surface-absorption potential, the same form of the imaginary potential was retained for this analysis of the low-energy data. The form of the potential is given by

$$V(r) = -Uf_r(r) - 4iA_iW_s(d/dr)[f_i(r)] + V_c, \quad (3)$$

where V_c is the Coulomb potential of a uniformly charged sphere of radius R_c. The form factor $f_r(r)$ is of the Woods-Saxon type

$$f_r(r) = \{1 + \exp[(r-R_r)A_r]\}^{-1}, \quad (4)$$

with the derivative of a similar form factor for the imaginary potential.

The first phase of this analysis was to fit the averaged angular distribution with the shape elastic cross sections predicted by the optical model. The geometric parameters were kept fixed at values used by Robinson *et al.*[6] The real radius R_r was chosen consistent with the electron-scattering data of Hahn *et al.*[11]

$$R_r = R(^{40}\text{Ca}) + R(\alpha) = (3.6+1.6)\ \text{F} = 5.2\ \text{F}.$$

[11] B. Hahn, D. G. Ravenhall, and R. H. Hofstadter, Phys. Rev. **101**, 1131 (1956).

Variations of the Coulomb radius parameter R_c were found to have very little effect even at these very low energies, so that the value of this parameter was fixed at 5.2 F. The values of the other parameters were as follows: $R_i = 5.0$ F, $A_r = 0.588$ F, and $A_i = 0.3$ F.

The quantity χ^2 was used as the criterion for describing the quality of the fits. Its definition has the usual form

$$\chi^2 = N^{-1} \sum_{i=1}^{N} \left(\frac{\sigma(\theta_i)_{\text{expt}} - \sigma(\theta_i)_{\text{calc}}}{\Delta\sigma(\theta_i)} \right)^2 . \quad (5)$$

Here N is the number of data points; $\sigma(\theta_i)_{\text{expt}}$, $\sigma(\theta_i)_{\text{calc}}$, and $\Delta\sigma(\theta_i)$ are the experimental cross section, the computed cross section, and the error in the experimental point, respectively, at the c.m. scattering angle θ_i.

The fits were, in general, unsatisfactory. At 5.5, 6.0, and 6.5 MeV the over-all fits might have been considered fair, in that the maximum value of χ^2 ranged from 3 to 5. However, the predicted cross sections were lower than the observed cross sections at the back angles. At these energies, the forward-angle scattering is primarily due to electrostatic rather than nuclear forces.

As the incident energy was increased the quality of the fits deteriorated rapidly. The calculated angular distributions exhibited much greater oscillations than was observed experimentally. The best fit obtained at 10.0 MeV is shown in Fig. 4. The potential strengths are $U = 142.0$ MeV and $W_s = 30.0$ MeV, and the value of χ^2 is 55.4. The calculated cross section is greater than the measured cross section up to a c.m. angle of about 130°. At angles greater than 158° the shape elastic scattering cross sections are consistently lower than the measure values. At 176°, it is only 25% of the observed value.

Even though the interaction is predominantly due to elastic-scattering mechanisms and the fluctuations have been removed by averaging, shape elastic scattering is not an adequate description of the experimental results. The nature of the discrepancy and the qualitative behavior of the data suggest that compound elastic scattering plays an important role.

B. Shape and Compound Elastic Scattering

To introduce compound elastic scattering, it is convenient to split the scattering amplitude S into two parts as suggested by Friedman and Weisskopf[12]:

$$S = \langle S \rangle + (S - \langle S \rangle) \quad (6)$$

The first term $\langle S \rangle$ is the shape elastic amplitude and is a smoothly varying function of energy. On the other hand, the compound elastic scattering described by the second term $(S - \langle S \rangle)$ varies over energy intervals of the order of the width of compound nuclear states.

[12] F. L. Friedman and V. F. Weisskopf, in *Niels Bohr and the Development of Physics*, Edited by Wolfgang Pauli (Pergamon Press, London, 1955), p. 134.

If the energy interval over which the averaging is carried out is small enough that the Coulomb scattering amplitude $f_c(\theta)$ and the relative Coulomb phase shift ω_l can be considered to be constants over this range, but large enough to justify the random-phase approximation (RPA), the cross section for compound elastic scattering is given by

$$d\sigma_{ce}/d\Omega=(1/4k^2)\sum_l(2l+1)^2[\langle|S_l|^2\rangle-|\langle S_l\rangle|^2]P_l^2(\cos\theta) \tag{7}$$

and that for shape elastic scattering by

$$d\sigma_{se}/d\Omega=|f_c(\theta)+(1/2ik)\sum_l(2l+1)(\langle S_l\rangle-1)\exp(2i\omega_l)P_l(\cos\theta)|^2, \tag{8}$$

so that

$$\langle d\sigma/d\Omega\rangle=(d\sigma_{se}/d\Omega)+(d\sigma_{ce}/d\Omega). \tag{9}$$

Here the symbols S_l are the elements of the scattering matrix. The effect of the RPA is to ignore all terms except those that are proportional to the absolute square of the scattering-matrix components. This approximation renders the compound elastic scattering incoherent with the shape elastic component.

From the computational point of view, it is convenient to express S_l in terms of the transmission coefficients T_l. This is easily carried out since

$$T_c=1-|\langle S_c\rangle|^2, \tag{10}$$

where the subscript c represents a particular channel. For the case of elastic scattering, the incoming and outgoing channels are identical so that we can represent S_l by S_{cc}.

Unitarity of the scattering matrix requires

$$\sum_{c'}\langle|S_{cc'}|^2\rangle=1, \tag{11}$$

so that

$$\langle|S_{cc}|^2\rangle=1-\sum_{c\neq c'}\langle|S_{cc'}|^2\rangle. \tag{12}$$

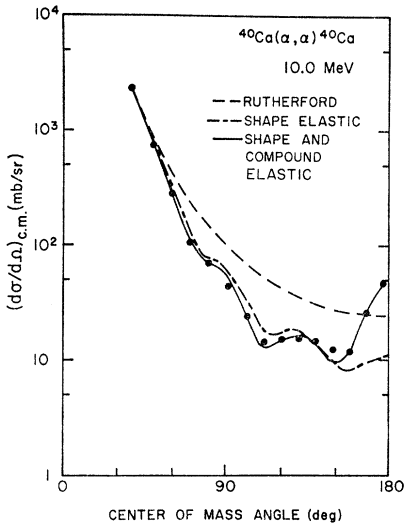

FIG. 4. Comparison of best fits at 10.0 MeV. The dot-dash curve is the best fit obtained with shape elastic cross section only. The solid line is the best fit obtained with the compound elastic contribution added to the shape elastic cross section. The Rutherford cross section is shown by the broken line.

Here $\sum_{c\neq c'}\langle|S_{cc'}|^2\rangle$ can be replaced by the expression obtained by Hauser and Feshbach,[13] viz.,

$$\sum_{c'\neq c}\langle|S_{cc'}|^2\rangle=T_c\sum_{c'\neq c}T_{c'}/\sum_{c''}T_{c''}, \tag{13}$$

where the sum over c'' is the sum over all exit channels. Hence the bracketed quantity in Eq. (7) becomes

$$\langle|S_{cc}|^2\rangle-|\langle S_{cc}\rangle|^2=1-\sum_{c'\neq c}\langle|S_{cc'}|^2\rangle-|\langle S_{cc}\rangle|^2$$
$$=T_c^2/\sum_{c''}T_{c''}. \tag{14}$$

The compound elastic-scattering cross section may now be written

$$d\sigma_{ce}/d\Omega=(1/4k^2)\sum_l(2l+1)^2(T_l^2/\sum_{c''}T_{c''})P_l^2(\cos\theta). \tag{15}$$

The effect of open channels, other than the elastic

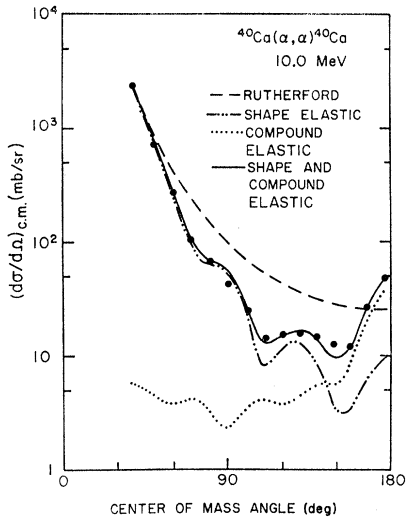

FIG. 5. Shape and compound elastic parts of the combined shape and compound elastic cross section at 10.0 MeV. The continuous curve is the best fit to the averaged data with shape elastic and compound elastic cross sections added together. The curve made up of dots and dashes is the contribution from shape elastic scattering, and the dotted curve is that from compound elastic scattering. The dashed line is a plot of the Rutherford cross section.

[13] W. Hauser and H. Feshbach, Phys. Rev. **87**, 366 (1952).

channel, is contained in the term $\sum_{c''} T_{c''}$. This quantity cannot, in general, be evaluated exactly when several channels are open. An approximate relation as given by Mayer-Kuckuk[14] is

$$\sum_{c''} T_{c''} = \rho(2l+1)\exp[-l(l+1)/2\sigma^2]. \quad (16)$$

This is based on the expression for the density of levels of spin l for the compound nucleus given by Bloch.[15] Here σ is the "spin-cutoff" factor and ρ is proportional to the level density for states with zero spin. The compound elastic cross section is therefore given by

$$\frac{d\sigma_{ce}}{d\Omega} = \frac{1}{4k^2}\sum_l \frac{(2l+1)T_l^2 P_l^2(\cos\theta)}{\rho\exp[-l(l+1)/2\sigma^2]}. \quad (17)$$

The procedure for fitting the data was as follows. The geometric parameters were kept fixed: $R_r = R_c = 5.2$ F,

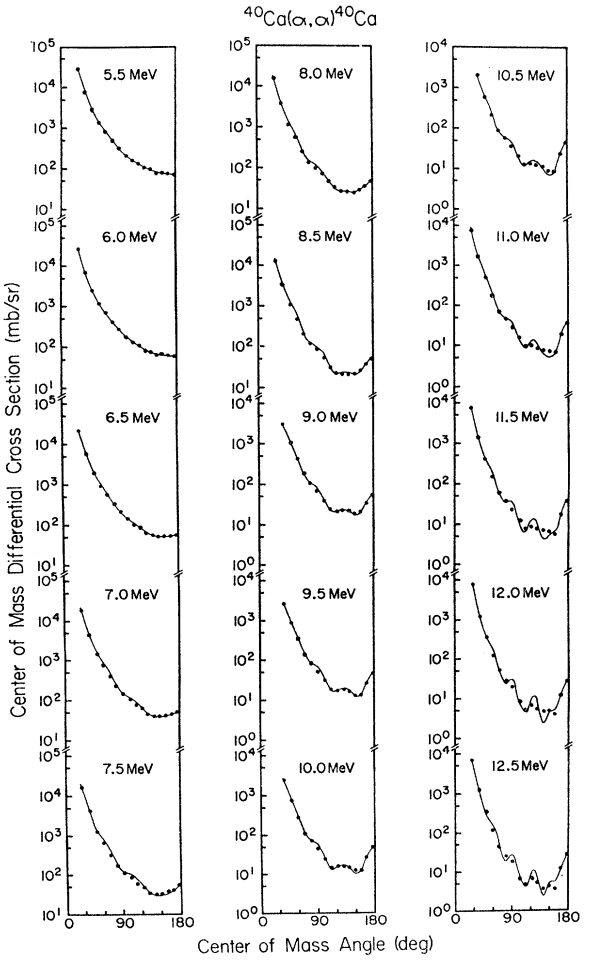

FIG. 6. Angular distributions from 5.5 to 12.5 MeV. The solid lines are optical-model fits obtained with the addition of a contribution from compound elastic scattering.

[14] T. Mayer-Kuckuk, in *Proceedings of Symposium on Recent Progress in Nuclear Physics with Tandems*, edited by W. Hering (Max-Planck Institute for Nuclear Physics, Heidelberg, 1966).
[15] C. Bloch, Phys. Rev. **93**, 1094 (1954).

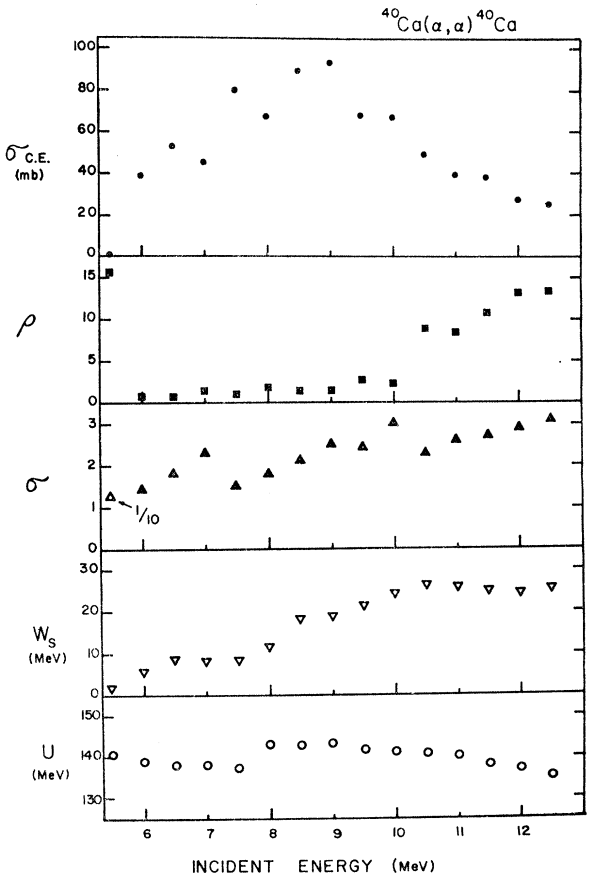

FIG. 7. The dependence of the real potential-well depth U, the strength of the surface imaginary potential W_s, the spin-cutoff factor σ, and the level density parameter ρ, on the incident energy of α particles. The compound elastic contribution σ_{ce} is displayed in the top section of the figure.

$R_i = 5.0$ F, $A_r = 0.59$ F, and $A_i = 0.3$ F. The search for the potential was confined to values in the vicinity of the phase-equivalent potential at 138 MeV. This selection is based on a comparison of the shell-model and cluster-model descriptions of the ground state of ^{44}Ti which is discussed by Robinson *et al.*[6]

Having fixed the geometry, the free parameters are U, W_s, σ, and ρ. A coarse grid search was performed first: U, 120–150 MeV in steps of 3 MeV; W_s, 0–50 MeV in steps of 5 MeV; σ, 1.0–60 in steps of two units; and ρ, 0.1–60 in steps of two units.

Angular distributions every 0.5 MeV were fitted using the above grid search. Values of U, W_s, σ, and ρ close to those corresponding to the local minimum of χ^2 were then scanned using a fine grid search: U, 1-MeV intervals over 10 MeV; W_s 2-MeV steps over 20 MeV; σ, 60 steps over six units; and ρ, 60 steps over 12 units.

Because the values of σ and ρ showed fluctuations as a function of bombarding energy, reflecting the fact that the values of U and W_s corresponding to minimum of χ^2 had not been precisely determined, extra fine grid searches were then performed in which U, W_s, σ, and ρ

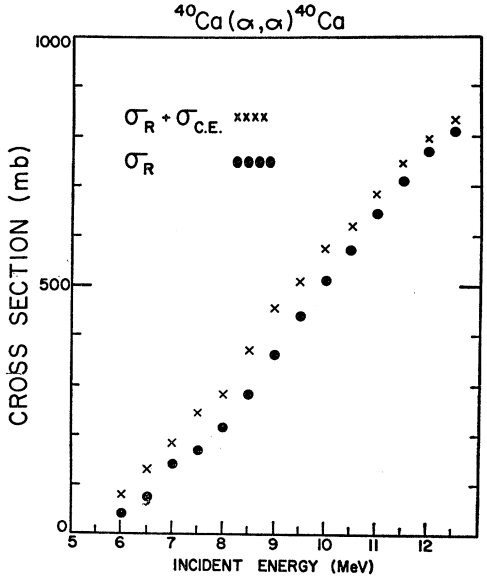

FIG. 8. Plots of the total reaction cross section $\sigma_R+\sigma_{ce}$ and of the nonelastic cross section σ_R as functions of bombarding energy.

were all varied in steps of 0.1 units around the local minimum.

The best fit obtained at 10.0 MeV using the Hauser-Feshbach and statistical-model formulation is compared to the best fit obtained including only shape elastic scattering in Fig. 4. In Fig. 5 the separate contributions from shape elastic scattering and compound elastic scattering are shown. The best fits obtained by this technique are shown in Fig. 6, in which angular distributions from 5.5 to 12.5 MeV are displayed.

IV. DISCUSSION OF RESULTS

The fits obtained at energies below 10.5 MeV are remarkably good. On the other hand, the quality of fits obtained above 10.5 MeV are relatively poor. This may be due, to a large extent, to the fact that at these energies the low-lying levels of ^{40}Ca can be excited by inelastic α-particle scattering. Above a bombarding energy of 10.5 MeV the inelastically scattered α particles have sufficient energy to pass nearly uninhibited across the Coulomb barrier. Inelastic scattering may then proceed without forming a compound nucleus. When this happens, the statistical approximation for treating the effect of all energetically allowed channels is no longer valid.

The final values of U, W_s, σ, and ρ are shown as a function of the bombarding energy in Fig. 7. The real potential strength U was found to be relatively constant. At 12.0 and 12.5 MeV, the values of U may be compared with the average value of U found by Robinson *et al.*,[6] and the agreement is good. The strength of the imaginary potential W_s has a value of 1.8 MeV at bombarding energy 5.5 MeV and gradually rises as the bombarding energy is increased. A rather rapid increase is observed in the vicinity of 7.5 MeV. This is probably due to the absorption of some of the incident flux by the ^{40}Ca$(\alpha, p)^{43}$Sc reaction. This reaction has a threshold at 3.89 MeV, and at 7.5 MeV the outgoing protons will have sufficient energy to penetrate the Coulomb barrier.

The spin-cutoff factor σ increases slowly with energy. From the simple relationship $l_{max}\approx kR$, an increase proportional to $\sqrt{E}$ can be expected. The level-density parameter ρ, which weights the contribution of the compound elastic scattering, increases slowly with energy. A rapid increase is noticeable around 10.5 MeV when the inelastic cross section first becomes significant.

The contribution of the compound elastic process is only 0.01 mb at 5.5 MeV, 38.6 mb at 6.00 MeV and increases to a maximum of 93.5 mb at 9.0 MeV. It then gradually decreases to 25 mb at 12.5 MeV. The slow increase in the compound elastic cross section may result from the increase in the penetration of the Coulomb barrier by the incident α particle with increasing energy. Above 9.0 MeV, the gradual decrease suggests that the competition from inelastic scattering allows fewer of the α particles absorbed into the compound nucleus to return to the elastic channel. Plots of the total reaction cross section $(\sigma_R+\sigma_{ce})$ and the nonelastic cross section σ_R as functions of energy are shown in Fig. 8.

ACKNOWLEDGMENTS

The authors are grateful to Dr. W. J. Thompson for numerous discussions. Dr. D. Robson suggested that the importance of the compound-elastic-scattering contribution be investigated and offered many helpful suggestions during the course of the analysis. The experiment was performed with the assistance of A. Bisson, J. Frickey, K. Knuth, W. Meyers, W. Wallace, and B. Watson.